(2)

Semiannual Report

Pseudomorphic Semiconducting Heterostructures from Combinations of AlN, GaN and Selected SiC Polytypes: Theoretical Advancement and its Coordination with Experimental Studies of Nucleation, Growth, Characterization and Device Development

Supported under Grant #N00014-90-J-1427
Department of the Navy
Office of the Chief of Naval Research
Report for the period January 1, 1992–June 30, 1992

Robert F. Davis, K. Shawn Ailey-Trent, Scott Kern, Young K. Kim,
Philip Grigg, Larry Rowland, Satoru Tanaka, and Cheng Wang
Materials Science and Engineering Department
North Carolina State University
Campus Box 7907
Raleigh, NC 27695-7907

June 1992

REPORT DOCUMENTATION PAGE

Form Approved
OMB No 0704-0188

1. AGENCY USE ONLY (Leave blank)	2. REPORT DATE	3. REPORT TYPE AND DATES COVERED
	June 1992	Semiannual 1/1/92–6/30/92

4. TITLE AND SUBTITLE
Pseudomorphic Semiconducting Heterostructures from Combinations of AlN, GaN and Selected SiC Polytypes: Theoretical Advancements and its Coordination with Experimental Studies

5. FUNDING NUMBERS
414s007---01
1114ss
N00179
N66005
4B855

6. AUTHOR(S)
Robert F. Davis

7. PERFORMING ORGANIZATION NAME(S) AND ADDRESS(ES)
North Carolina State University
Hillsborough Street
Raleigh, NC 27695

8. PERFORMING ORGANIZATION REPORT NUMBER
N00014-90-J-1427

9. SPONSORING / MONITORING AGENCY NAME(S) AND ADDRESS(ES)
Department of the Navy
Office of the Chief of Naval Research
800 North Quincy, Code 1513:CMB
Arlington, VA 22217-5000

10. SPONSORING / MONITORING AGENCY REPORT NUMBER

11. SUPPLEMENTARY NOTES

12a. DISTRIBUTION / AVAILABILITY STATEMENT
Approved for Public Release—Distribution Unlimited

12b. DISTRIBUTION CODE

13. ABSTRACT (Maximum 200 words)

As an initial step toward the achievement of pseudomorphic heterostructures of nitride materials, thin films of an undoped and p-type doped $Al_xGa_{1-x}N$ solid solution as well as InN have been successfully deposited using a modified gas source MBE system. Application of single layers of the $Al_xGa_{1-x}N$ solid solution or pure GaN films as UV light photon detectors has been achieved. The gain exhibited by these detectors at a forward voltage of 5V was 500μA and 10 mA for the solid solution films deposited on sapphire and α(6H)-SiC substrates, respectively. The GaN film deposited on sapphire exhibited a gain of 20μA. Solid solutions and multilayers of AlN and SiC have also been grown on 6H-SiC (0001) substrates cut 3–4° off-axis to [11$\bar{2}$0]. Evidence is presented which suggests that the AlN-rich solid solutions are cubic. Pseudomorphic heterostructures of 6H-SiC, 2H-AlN, and 3C-SiC have been produced for the first time. Each of the layers was monocrystalline, and the interfaces were chemically and structurally sharp and reasonably smooth. Moreover, each layer represents a different crystal structure and bandgap energy. In concert with this research, we are also investigating the chemical interdiffusion of AlN and SiC. Initial results indicate that the interdiffusivity of the four elements is $\approx 10^{-14}$ cm^2/hr. Finally, initial research concerned with the BN on polycrystalline CVD diamond is reported.

14. SUBJECT TERMS	15. NUMBER OF PAGES
pseudomorphic heterostructures, (AlGa)N solid solutions, SiAlCN solid solutions, indium nitride, alpha (6H)-silicon carbide, gallium nitride, aluminum nitride, gas-source molecular beam epitaxy, cubic boron nitride, diamond	31
	16. PRICE CODE

17. SECURITY CLASSIFICATION OF REPORT	18. SECURITY CLASSIFICATION OF THIS PAGE	19. SECURITY CLASSIFICATION OF ABSTRACT	20. LIMITATION OF ABSTRACT
UNCLAS	UNCLAS	UNCLAS	SAR

Table of Contents

I. Introduction

The advent of techniques for growing semiconductor multilayer structures with layer thicknesses approaching atomic dimensions has provided new systems for both basic physics studies and device applications. Most of the research involving these structures has been restricted to materials with lattice constants that are equal within $\simeq 0.1\%$ However it is now recognized that interesting and useful pseudomorphic structures can also be grown from a much larger set of materials that have lattice-constant mismatches in the percent range. Moreover, advances in computer hardware and software as well as the development of theoretical structural and molecular models applicable for strained layer nucleation, growth and property prediction have occurred to the extent that the field is poised to expand rapidly. It is within this context that the research described in this report is being conducted. The materials systems of concern include combinations of the direct bandgap materials of AlN and GaN and selected, indirect bandgap SiC polytypes.

The extremes in thermal, mechanical, chemical and electronic properties of SiC allow the types and numbers of current and conceivable applications of this material to be substantial. However, a principal driving force for the current resurgence of interest in this material, as well as AlN and GaN, is their potential as hosts for high power, high temperature microelectronic and optoelectronic devices for use in extreme environments. The availability of thin film heterostructural combinations of these materials will substantially broaden the applications potential for these materials. The pseudomorphic structures produced from these materials will be unique because of their chemistry, their wide bandgaps, the availability of indirect/direct bandgap combinations, their occurrence in cubic and hexagonal forms and the ability to tailor the lattice parameters and therefore the amount of strain and the physical properties via solid solutions composed of the three components.

The research described in the following subsections constitutes the second reporting period involving material growth in this program following a prolonged period of equipment fabrication, testing and reconfiguration. Specifically, $Al_xGa_{1-x}N$ films have been successfully deposited via gas source molecular beam epitaxy (GSMBE) as a prelude to producing multilayer heterostructures involving two AlN/GaN alloys and/or a binary nitride and an alloy. Our first attempts regarding the growth of InN were also pursued in this reporting period. In addition, heterostructures and solid solutions of AlN/SiC have been grown on α(6H)-SiC (0001). Related studies concerned with the chemical interdiffusion of AlN and SiC have been conducted in tandem with the growth experiments to determine the extent and nature of the solid solubility of these two components. Finally, initial studies involving the pseudomorphic growth of cubic-BN on diamond have been initiated. The following subsections detail the procedures, results, discussions of these results, conclusions and plans for future research. Each subsection is self-contained with its own figures, tables, and references.

II. Deposition of $Al_xGa_{1-x}N$ Solid Solution and InN Films

A. Introduction

Group III-V nitrides are promising candidates for optoelectronic devices, such as light emitting diodes and semiconductor lasers in the blue and ultraviolet regions of the spectrum [1]. It is believed that, like the highly successful As-based and P-based materials, the heterostructures of the III-V nitrides (heterostructure quantum wells or even superlattice quantum wells) will become increasingly important for optoelectronic device applications. The advantages of heterostructures, such as i) enhanced carrier mobility & improved device speed, ii) engineered bandgap to produce suitable lasing wavelengths, and iii) greatly enhanced quantum efficiency (carrier confinement in radiative region and a window to the emitted radiation) will enhance device performance.

For real device application, research concerned with single III-V nitrides material is still in its initial stages. However, it is very important to study heterostructure III-V nitrides in advance, in order to meet the needs of future device structure. Our early success in depositing AlN/GaN multilayer films has shown that using modified gas source MBE system, heterostructural films having sharp interfaces both chemically and structurally, as well as good crystal quality [2] could be obtained. Based on these results, we have also initiated research efforts to make a variety of different solid solution materials. This will extend the flexibility of future heterostructural device designs. In the following, the preliminary research results on deposition of $Al_xGa_{1-x}N$ solid solution and InN films are reported. In addition, the results of preliminary device applications of GaN and $Al_xGa_{1-x}N$ solid solution films in UV light photon detectors will be presented.

B. Experimental Procedure

The thin film deposition system employed in this research was a commercial Perkin-Elmer 430 MBE system. This system consisted of three parts: a load lock (base pressure of $5 * 10^{-8}$ Torr), a transfer tube (base pressure of 1×10^{-10} Torr), which also was used for degas the substrates, and the growth chamber (base pressure of $5 * 10^{-11}$ Torr). Knudson effusion cells with BN crucibles and Ta wire heaters were charged with 7N pure gallium, 6N pure aluminum, indium and magnesium. Ultra-high purity nitrogen, further purified by a chemical purifier, was used as the sources gas. It was excited by an ECR plasma source, which was designed to fit inside the 2.25 inch diameter tube of the source flange cryoshroud. The details of the system can be found elsewhere [3].

The substrates were (0001) oriented α(6H)-SiC and epitaxial quality sapphire wafers. Prior to loading into the chamber, the a-SiC substrates were cleaned by standard degreasing and RCA cleaning procedure. The sapphire substrates were cleaned using the following

procedures: degreasing and DI water rinse, 10 minutes in a hot solution of HPO_3:H_2SO_4 with 1:1 ratio, DI water rinse thoroughly, finally dip in 1:10 solution of 49% HF:H_2O. All cleaned substrates were then mounted on a 3 inch molybdenum block and load into the system. After undergoing a degassing procedure (700°C for 30 minutes), the substrates were transfer into the deposition chamber. Finally RHEED was performed to examine the crystalline quality of the substrates.

C. Results

1. Deposition of $Al_xGa_{1-x}N$ Solid Solutions

The goal in this aspect of the research has been the deposition of films of $Al_xGa_{1-x}N$ solid solution films for x ranging from 1 to 0. Compositional ratios of Al-atoms to the Ga-atoms in the films were varied through control of the Ga-cell and Al-cell temperatures. Typical deposition conditions are listed in Table I. RHEED was used to examine the crystalline quality of the films. It showed that all the films for x ranging from 1 to 0 were monocrystalline. The real Al/Ga compositional ratios in the alloy films were determined using a Scanning Auger Microprobe (SAM). The results indicated that the real Al/Ga composition ratios were close to the estimated ratios based on Al/Ga flux ratios. A multilayer film which consisted of seven $Al_xGa_{1-x}N$ sublayers was deposited. The values of x in the various sublayers were 1, 0.7, 0.5, 0.3, 0.2, 0.12 and 0. The RHEED pattern of the top GaN film indicated that film had a good crystalline quality.

Table I. Deposition Conditions for Undoped $Al_xGa_{1-x}N$ Films.

Nitrogen pressure	2×10^{-4} Torr
Microwave power	50W
Gallium cell temperature	945~990°C
Aluminum cell temperature	1120~1030°C
substrate temperature	650°C

2. Optical Device Applications of GaN and $Al_{0.12}Ga_{0.88}N$ Films

We have also characterized the GaN and $Al_xGa_{1-x}N$ solid solution films in terms of the ir optoelectronic properties. Simple UV light photon detectors have been produced and tested. Single crystal GaN or $Al_{0.12}Ga_{0.88}N$ films having a thickness of ≈3000 Å were first deposited on α-SiC and sapphire substrates using the deposition conditions discussed above. A 1000Å thick Al layer was then in-situ deposited on top of the films at a temperature of

200°C. The top Al layer was further masked and etched by lithographic techniques to form interdigitated electrode configuration. Figure 1 is a schematic illustration of a device of this type. Current-voltage (IV) measurements in both dark and illuminated states were performed to characterize these devices. A 500 W high pressure Hg arc-lamp with a collimating lens (Oriel model 6285), was used as the ultra-violet illumination source. Figure 2 shows the results of the IV characterization for three of the photon detectors fabricated in this research.

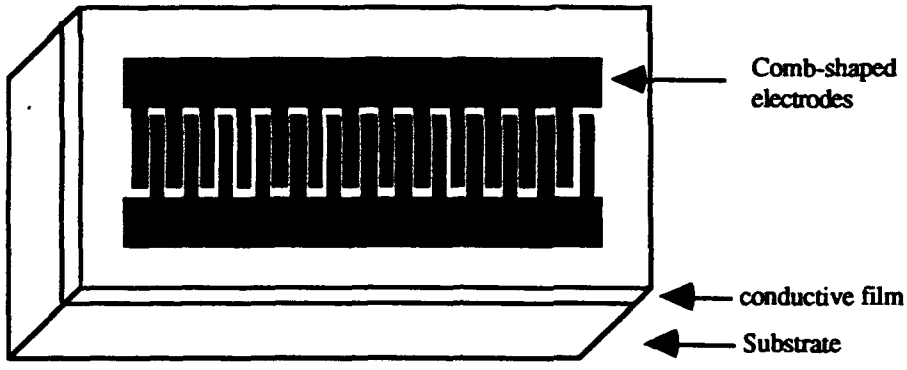

Figure 1. Schematic illustration of the photoconductive photon detector devices fabricated as described in the text.

These results show that all three detectors exhibited moderately good photoresponse to the UV illumination. The gain of each of the detectors, defined as

$$G = \text{light current} / \text{dark current}$$

was about the same: 10~20 at a bias voltage of 5 volts, even though the photocurrents for the $Al_{0.12}Ga_{0.88}N$ detectors were much larger than for the GaN detector. At a bias voltage of 5 volts, photocurrents of as large as 10 mA were obtained for the $Al_{0.12}Ga_{0.88}N$ detector on a sapphire substrate.

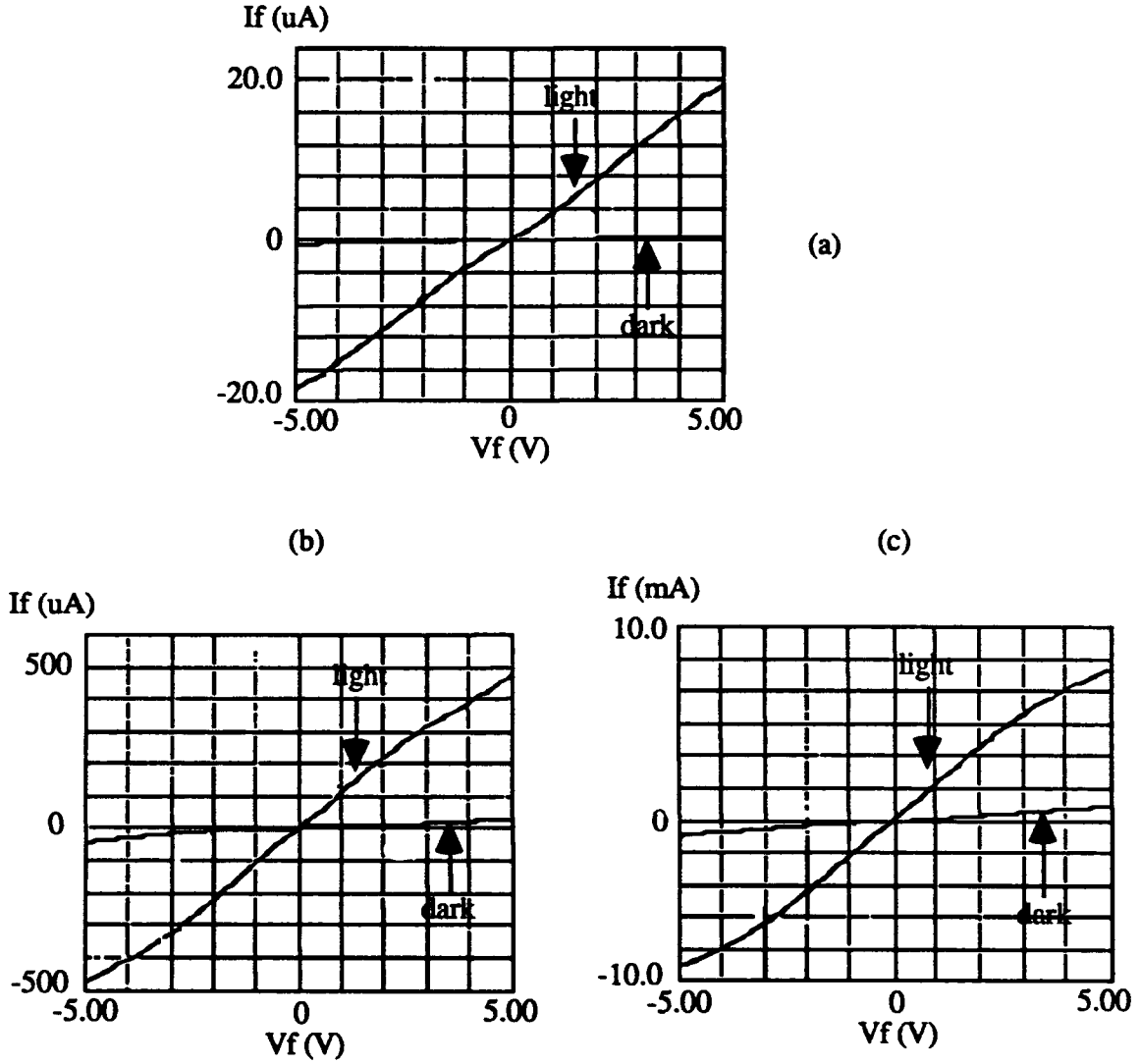

Figure 2. IV measurements for three UV light photon detectors with a photoconductive layer of (a) GaN on sapphire; (b) $Al_{0.12}Ga_{0.88}N$ on sapphire; and (c) $Al_{0.12}Ga_{0.88}N$ on alpha (6H)-SiC substrates.

3. Deposition of P-type $Al_{0.12}Ga_{0.88}N$ Film

The electrical properties of the $Al_xGa_{1-x}N$ alloy films were difficult to measure, since they were very resistive. As such, p-type doping of these films with Mg has been investigated. Table II lists the deposition conditions for growth and doping of these films. A ≈200Å AlN buffer layer was deposited after exposing the Al coated substrates to the nitrogen plasma for 5 minutes. Finally, the Mg-doped GaN films were deposited. This procedure was used to prevent any amorphous interfacial layer forming at the interface of substrate and film. The van der Pauw resistivity and Hall effect measurements indicated that this Mg-doped $Al_{0.12}Ga_{0.88}N$ film was a p-type with a resistivity of 10 Ω·cm and a low hole mobility.

Table II. Deposition Conditions for Mg-doped $Al_{0.12}Ga_{0.88}N$ Films.

Nitrogen pressure	$2*10^{-4}$ Torr
Microwave power	50W
substrate temperature	650°C
Gallium cell temperature	980°C
Aluminum cell temperature	1030°C
Magnesium cell temperature	300°C
Al layer	2 monatomic layer
AlN buffer layer	150~200Å
Mg-doped $Al_{0.12}Ga_{0.88}N$	4000~5000Å

4. Deposition of InN Films

With a direct bandgap of 1.95 eV, InN is very attractive for use in the formation of solid solution films with AlN (bandgap of 6.28 eV). Bandgaps of solid solution films could be engineered from 1.95 eV (visible range), up to the deep UV range of 6.28 eV. It would give considerable flexibility to the heterostructural device design. However, InN has been the least studied of all the III-V nitride materials. The fact that the equilibrium N vapor pressure for InN is much higher than for other nitrides often results in highly conducting films. Also, no deposition of $Al_xIn_{1-x}N$ films has ever been reported. Recently, T. Matsuoka et. al. reported that single crystalline InN films have been grown by using low deposition temperatures and higher N/In ratios in their MOVPE system [4]. The initial results of our research concerned with the deposition of InN films by our modified source gas MBE system are reported below.

The deposition conditions listed in Table III are typical for InN deposition. Alpha (6H)-SiC and sapphire, both oriented (0001), were used as the substrates. To reduce the lattice mismatch, an AlN buffer layer was deposited before the InN deposition. The resulting films possessed a mirror-surface. The crystalline quality of the surface was examined by RHEED; the surface morphology was examined using SEM.

As indicated in Figure 3, RHEED taken in the <2$\bar{1}$$\bar{1}$0> azimuth of films, showed the deposited InN films on both alpha (6H)-SiC and sapphire substrates to be single crystalline films. An SEM picture for an InN film deposited on AlN/α(6H)-SiC, shown in Figure 4, indicated the film had a very smooth surface. No In droplets have been found. The electrical properties of these InN films are currently being investigated and will be reported later.

Table III. Deposition Conditions for InN Films.

Nitrogen pressure	$2*10^{-4}$ Torr
Microwave power	50W
Indium cell temperature	~800°C
AlN buffer layer	150~200Å deposited at 650°C
InN	deposited at 500°C

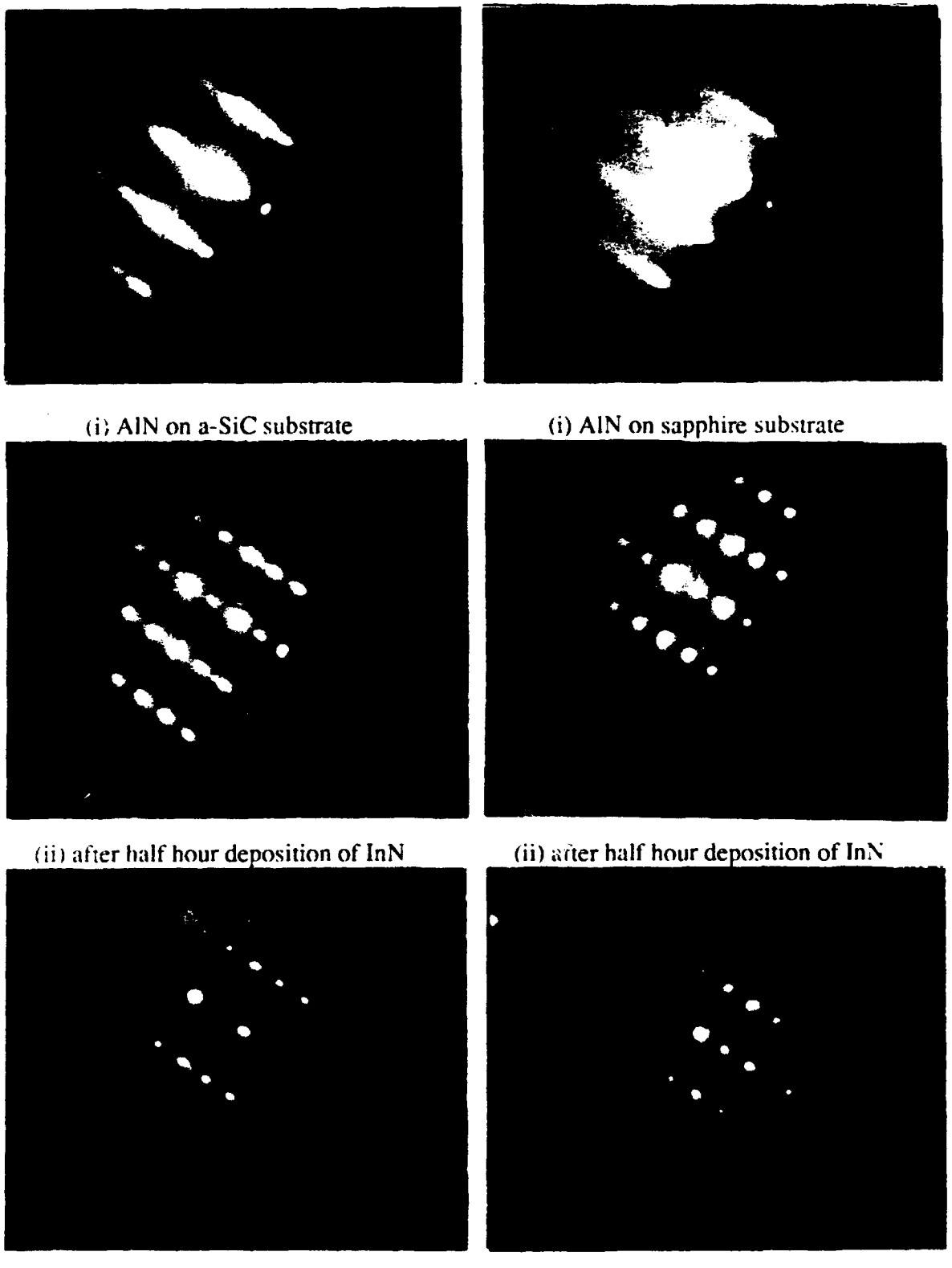

Figure 3. RHEED patterns for the films deposited on (a) vicinal α(6H)-SiC (0001) and (b) sapphire (0001).

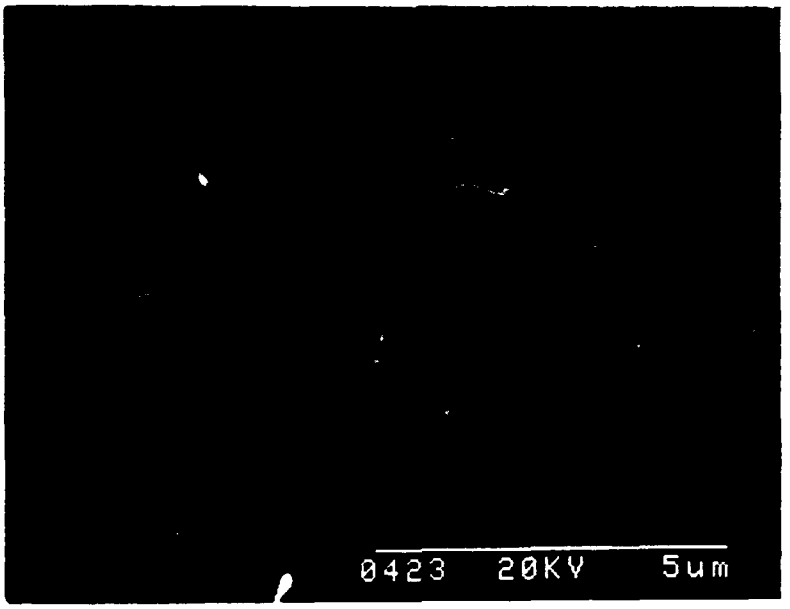

Figure 4. Surface morphology of an InN film obtained using by SEM.

D. Summary

Using our modified gas source MBE system, $Al_xGa_{1-x}N$ solid solution films, p-type $Al_{0.12}Ga_{0.88}N$ films and InN films have been successfully deposited. Sample uv detectors made from the GaN and $Al_xGa_{1-x}N$ solid solution films have been tested. Results showed that III-V nitrides films can be used as UV light photon detectors, although much more research must be conducted to meet the needs of device designers.

E. Future Research Plan

We have shown that $Al_xGa_{1-x}N$ solid solution films can be made in our modified gas source MBE system. These solid solution films were also used as the photoconductive material in the photon detectors. However, much more work still need to be done. To achieve higher gain in the detectors, the films must be further optimized. Recently, we have found that the GaN films with improved crystal quality can be obtained if the thin amorphous interfacial layer on the substrate caused by interaction with the nitrogen plasma is eliminated. We have also showed that we can produce p-type $Al_{0.12}Ga_{0.88}N$ films by this deposition procedure. The application of undoped $Al_xGa_{1-x}N$ films with better crystal quality will again be studied in terms of photon detector devices. Secondly, more device properties, such as response time, will be characterized

With the ability to obtain p-type $Al_xGa_{1-x}N$ solid solution films, we will now concentrate our research effort toward heterostructural device application. We will also continue to study the growth and characterization of InN, to determine the conditions for achieving $Al_xIn_{1-x}N$ solid solution films.

F. References

1. R. F. Davis, "Current Status of the Research on III-V Mononitrides Thin Films for Electronic and Optoelectronic Applications," in The *Physics and Chemistry of Carbides, Nitrides and Borides*, R. Freer, ed. Kluwer Academic Publishers, Dordrecht, The Netherlands, 1990, pp. 653-669.
2. Z. Sitar, M. J. Paisley, B. Yan, J. Ruan, J. W. Choyke and R. F. Davis, J. Vac. Sci. Technol. B **8**, 316 (1990).
3. Z. Sitar, M. J. Paisley, D. K. Smith and R. F. Davis, Rev. Sci. Instrum. **61**, 2407 (1990).
4. T. Matsuoka, T. Sasaki and A. Katsui, Optoelectronics **5**, 53 (1990).

III. Deposition and Characterization of AlN/SiC Solid Solutions and Pseudomorphic Heterostructures

A. Introduction

Silicon carbide (SiC) is a wide bandgap material that exhibits polytypism, a one-dimensional polymorphism arising from the various possible stacking sequences of the silicon and carbon layers. The lone cubic polytype, β-SiC, crystallizes in the zincblende structure and is commonly referred to as 3C-SiC. In addition, there are also approximately 250 other rhombohedral and hexagonal polytypes [1] that are all classed under the heading of α-SiC. The most common of the α-SiC polytypes is 6H-SiC.

Beta-SiC is finding considerable use in applications that utilize its attractive physical and electronic properties such as wide bandgap (2.2 eV at 300K) [2], high breakdown electric field (2.5×10^6 V/cm) [3], high thermal conductivity (3.9 W/cm °C) [4], high melting point (3103K at 30 atm) [5], high saturated drift velocity (2×10^7 m/s) [6], and small dielectric constant (9.7) [7]. Primarily due to its larger electron mobility than that of the hexagonal polytypes, such as 6H-SiC [8], β-SiC is preferable to hexagonal SiC for most device applications.

Aluminum nitride (AlN) is of particular interest at this time because of its very large bandgap. It is the only intermediate phase in the Al-N system and normally forms in the wurtzite (2H-AlN) structure. Most current uses of AlN center on its mechanical properties, such as high hardness (9 on Mohs scale), chemical stability, and decomposition temperature of about 2000°C [9]. Properties such as high electrical resistivity (typically $\geq 10^{13}$ Ω-cm), high thermal conductivity (3.2 W/cm K) [10], and low dielectric constant ($\varepsilon \approx 9.0$) make it useful as a potential substrate material for semiconductor devices as well as for heat sinks. The wurtzite form has a bandgap of 6.28 eV [11] and is a direct transition, thus it is of great interest for optoelectronic applications in the ultraviolet region.

The interest in wide bandgap semiconductors has increased greatly in the past few years [12,13]. The reasons for this expanded interest can be attributed to many factors. Because of the physical properties of wide bandgap, novel devices with properties superior to those made from either gallium arsenide or silicon should be possible. For example, wide bandgaps are required for high temperature, high power, or high frequency applications as well as short wavelength optoelectronic applications. In addition, the II-VI compounds (tellurides and selenides of cadmium and zinc), which in the past were considered the primary materials for such applications, have documented doping problems [14]. Two of the most important wide bandgap materials are the aforementioned, SiC and AlN.

Because of the difference in bandgaps (2.28 eV for 3C-SiC and 6.28 eV for 2H-AlN) between the materials, a considerable range of wide bandgap materials, made with these

materials, should be possible. Two procedures for bandgap engineering are solid solutions and multilayers. A particularly important factor is that the two materials have a lattice mismatch of less than one percent.

Research in ceramic systems suggests that complete solid solubility of AlN in SiC may exist [15]. Solid solutions of the wurtzite crystal structure should have E_g from 3.33 eV to 6.28 eV at 0 K. Although it has not been measured, the bandgap of cubic AlN has been estimated to be around 5.11 eV at absolute zero and is believed to be indirect [16]. Cubic solid solutions should thus have E_g from 2.28 eV to roughly 5.11 eV at 0 K and would be indirect at all compositions if theory holds true.

Because of their similarity in structure and close lattice and thermal match, AlN-SiC heterostructures are feasible for electronic and optoelectronic devices in the blue and infrared region. Monocrystalline AlN layers have been formed by CVD on SiC substrates [17] and SiC layers have been formed on AlN substrates formed by AlN sputtering on single crystal W [18]. In addition, theory on electronic structure and bonding at SiC/AlN interfaces [16] exists and critical layer thicknesses for misfit dislocation formation have been calculated for cubic AlN/SiC [19]. Note that AlN (at least in the wurtzite structure) is a direct-gap material and SiC is an indirect gap material. Superlattices of these materials would have a different band structure than either constituent element. The Brillouin zone of a superlattice in the direction normal to the interfaces is reduced in size. This reduction in zone size relative to bulk semiconductors causes the superlattice bands to be "folded into" this new, smaller zone. This folding can cause certain superlattice states to occur at different points in k space than the corresponding bulk material states [20]. This can lead to direct transitions between materials which in the bulk form have indirect transitions. This has been demonstrated in the case of $GaAs_{0.4}P_{0.6}$/GaP and $GaAs_{0.2}P_{0.8}$/GaP superlattices, where both constituents are indirect in the bulk form [21]. Whether this is possible in the case of AlN/SiC is unknown, but very intriguing. It may be possible to obtain direct transitions throughout nearly the entire bandgap range with use of superlattices of AlN and SiC. Use of solid solutions in superlattices introduces additional degrees of freedom. For example, the bandgap can be varied independently of lattice constant with proper choice of layer thickness and composition if superlattices of solid solutions of AlN and SiC were formed.

Due to the potential applications of solid solutions and superlattice structures of these two materials, a MBE/ALE system was commissioned, designed, and constructed for growth of solid solutions and heterostructures of these two materials. In this report, we present evidence that suggests the formation of cubic solid solutions of AlN and SiC as well as evidence of monocrystalline AlN and SiC heterostructure layers on 6H-SiC (0001) substrates cut 3-4° off-axis toward [11$\bar{2}$0].

B. Experimental Procedure

These films were grown on Si faces of 6H-SiC (0001) substrates provided by Cree Research, Inc. The substrates used in this study were found to be off-axis (3-4° off (0001) toward [11$\bar{2}$0]) by X-ray diffraction using the Laue back-reflection method. Films were grown using the MBE system detailed in previous reports, and readers are referred to these reports for a description and schematic of the system. Sources used are as follows: disilane (Si_2H_6) for silicon, ethylene (C_2H_4) for carbon, gaseous nitrogen (N_2) introduced through an ASTeX Compact ECR electron cyclotron resonance (ECR) plasma source for nitrogen, and an MBE effusion cell for evaporation of solid aluminum. Samples were chemically cleaned prior to growth in a 10% HF solution for 5 min, followed by a DI water rinse for 2 min. All of the experiments were done in excess of 1000°C, thereby desorbing any hydrocarbons or oxide layers from the SiC surface.

1. Solid Solution Procedure

Solid solutions of SiC and AlN were formed by GSMBE on the 6H-SiC substrates using the following conditions: Si_2H_6 flow, 0.1 sccm; C_2H_4 flow, 0.2 sccm; N_2 flow "diluted" with argon (about a 10:1 Ar to N_2 ratio) to an operating pressure of 1.6×10^{-4} torr; Al source temperature, 1050°C; sample temperature, 1050°C; and time, 240 minutes. Pressures during growth typically reached 2×10^{-4} torr, with the system base pressure being less than 1×10^{-9} torr.

Reflection high-energy electron diffraction (RHEED) was used to determine the crystalline quality of the surface of the resultant films. In addition, the chemical composition and depth profile of each sample were obtained using a scanning Auger microprobe. Because the films were very thin (<100 Å) and polycrystalline, no further analysis was performed.

2. Multilayer Procedure

Superlattices, or multilayers, of SiC and AlN were formed by GSMBE on the 6H-SiC substrates using the following conditions. First, the AlN layers were grown using the following conditions: Al source temperature, 1210°C; N_2 flow to an operating pressure of 1.6×10^{-4} torr; and time, 20 minutes. Next, the SiC layers were grown using the following conditions: Si_2H_6 flow, 0.1 sccm; C_2H_4 flow, 0.2 sccm and time, 150 minutes. The entire growth run was performed with a sample temperature of either 1050°C or 1200°C. Pressures during growth typically reached 2×10^{-4} torr, with the system base pressure being less than 1×10^{-9} torr.

Reflection high-energy electron diffraction (RHEED) was used to determine the crystalline quality of the surface of the resultant films. Those films that were monocrystalline by RHEED were further analyzed. The chemical composition and depth profile of each sample were obtained using a scanning Auger microprobe. A field-emission scanning

electron microscope (SEM) was used to observe surface morphology. And, high-resolution transmission electron microscopy (HRTEM) was employed to determine the defects and crystalline structure present in the film as well as examining the film/interface region. An Ashaki EM-002B HRTEM was used for this purpose.

C. Results

1. Solid Solutions

Figure 1 shows a RHEED photograph of an AlN-SiC sample grown under the procedure described above. Note that the pattern consists of both spots and rings. The spots correspond to a [110] zone axis in the cubic system. The rings, which are invariant with respect to orientation, indicate that the film is polycrystalline:

Figure 1. RHEED image of an AlN-SiC solid solution on a 6H-SiC substrate taken after growth.

An Auger depth profile of the AlN-SiC film is shown in Figure 2. As the graph indicates, the film is about 72% AlN and 28% SiC. It is also important to note that the amount of carbon in the film is lower throughout the film despite being added in a 2:1 ratio to silicon. Also, since the sputtering rate was approximately 90 Å/min, the thickness of this film can be roughly estimated as about 80 Å.

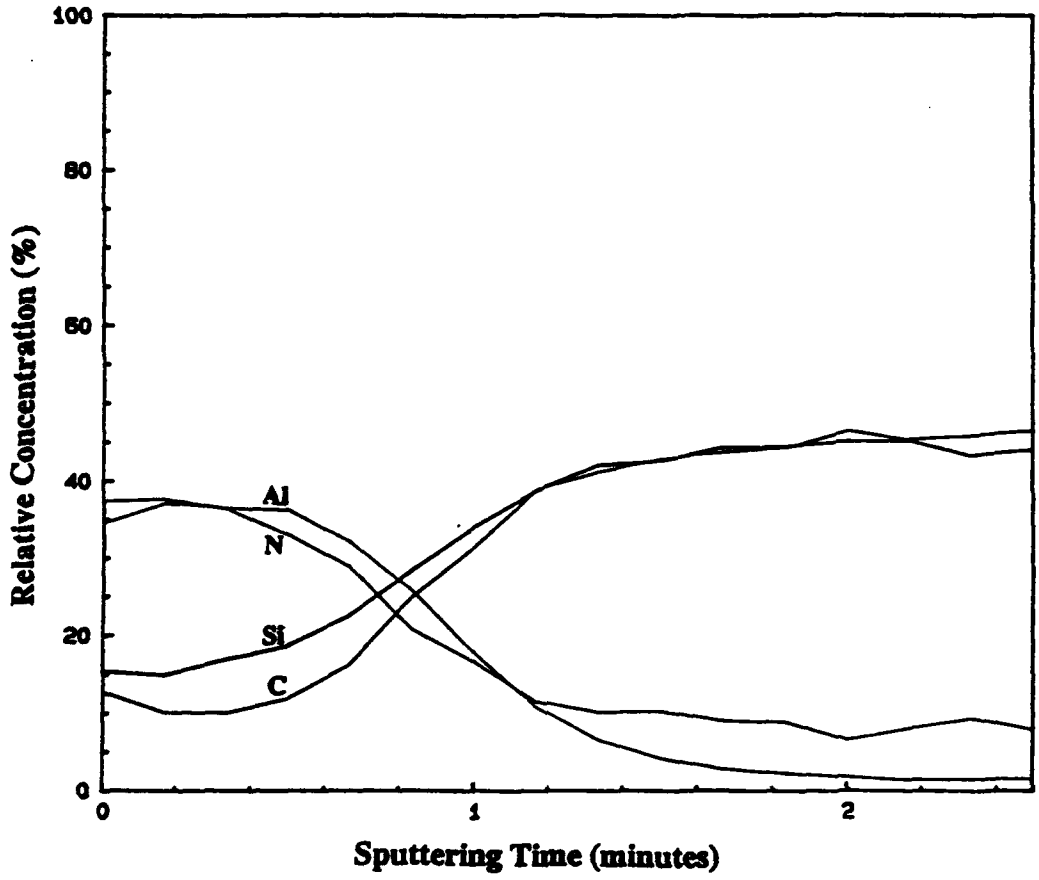

Figure 2. Auger plot of relative concentration vs. time for an AlN-SiC solid solution film.

2. Multilayers

Figure 3 shows an HRTEM image of a layer of AlN grown onto a 6H-SiC substrate. The inset of the photograph shows a diffraction pattern for the AlN region. The diffraction pattern identifies this AlN layer as being a single crystal, wurtzite (2H) structure. Note that the AlN surface appears very wavy and rough.In addition, the film-substrate interface is very disordered. Obviously, this layer would not be satisfactory for multilayer thin films.

In an attempt to improve film quality, further studies were done to find the optimum temperature for multilayer growth. This was found to be 1050°C and Figure 4 shows an Auger plot of such a multilayer. The SiC is found to be stoichiometric and about 160 Å thick. The relative concentrations of Al and N in the AlN layer correspond well to those obtained from a standard for AlN that was shown in the previous report indicating it to be stoichiometric. This layer is about 70 Å thick.

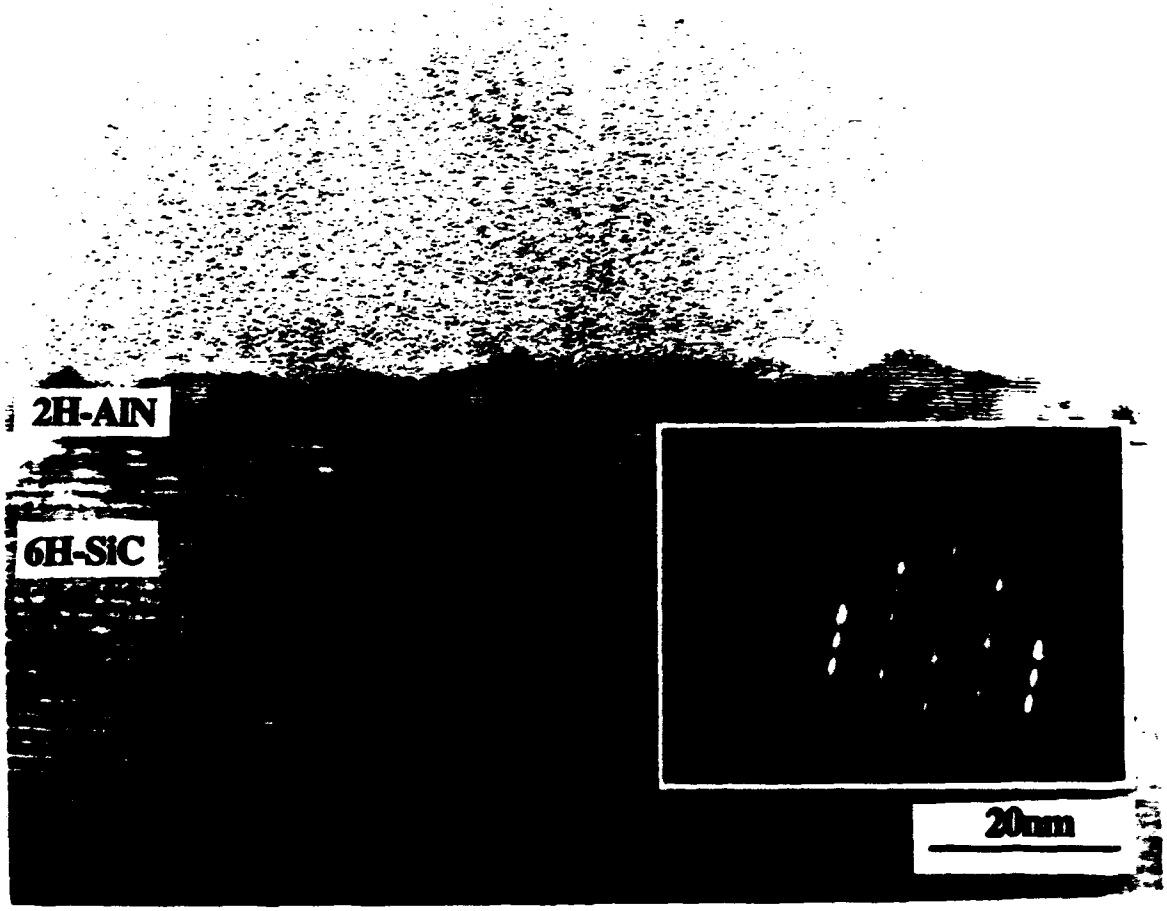

Figure 3. Cross-sectional HRTEM image of 2H-AlN film and 6H-SiC substrate. Inset: Diffraction pattern for the AlN layer indicates a 2H (wurtzite) structure.

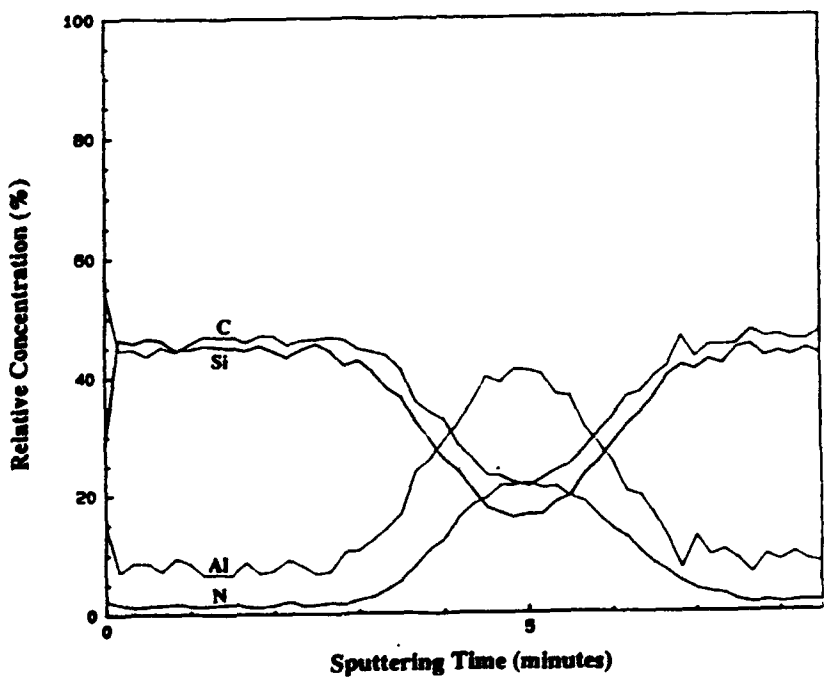

Figure 4. Auger plot of relative concentration vs. time for an AlN-SiC multilayer.

Figure 5 shows a RHEED photograph of the top (SiC) layer of this heterostructure taken after growth. The pattern is characteristic of a [$2\bar{1}\bar{1}0$] zone axis in the cubic system.The pattern also indicates that the SiC layer is a single crystal. Refer to Figure 3 for the diffraction image of 2H-AlN.

Figure 6 shows the surface morphology of the SiC top layer. The surface appears very smooth except for widely spaced, faceted imperfections 0.5-1.0 μm across. The remaining film appears smooth at high magnification.

An HRTEM photograph of this multilayer is shown in Figure 7. There are three structures present in the layering scheme--3C- and 6H-SiC and 2H-AlN. The interface between the substrate and the AlN layer is far superior to that shown in Figure 3. This interface is good except around the surface stepson the substrate. At these steps, there is a strain field that perpetuates itself throughout the film as noted by the contrast around the steps in the photograph. The actual AlN later shows a much better thickness uniformity than the layer shown in Figure 3 grown 150°C higher. The interface between the 2H-AlN and the 3C-SiC layers is also very good. However, the SiC layer itself shows stacking faults, microtwins, and poor thickness uniformity.

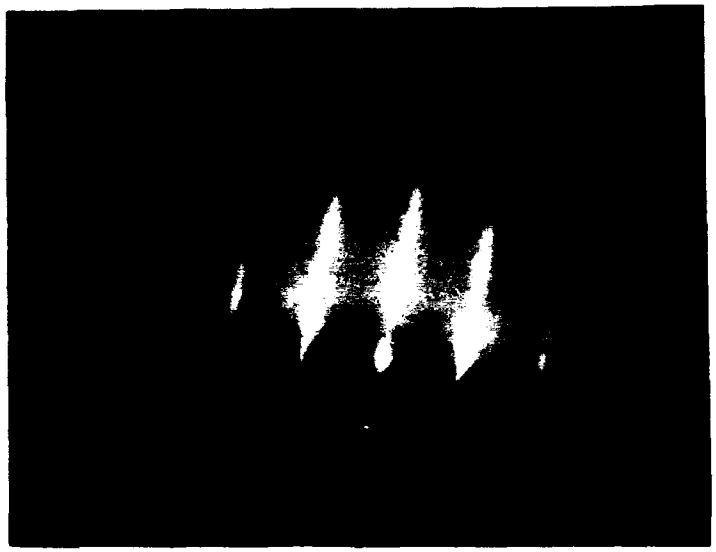

Figure 5. RHEED image of an AlN-SiC multilayer on a 6H-SiC substrate taken after growth.

Figure 6. Surface morphology of the top layer (SiC) of a multilayer film by scanning electron microscopy

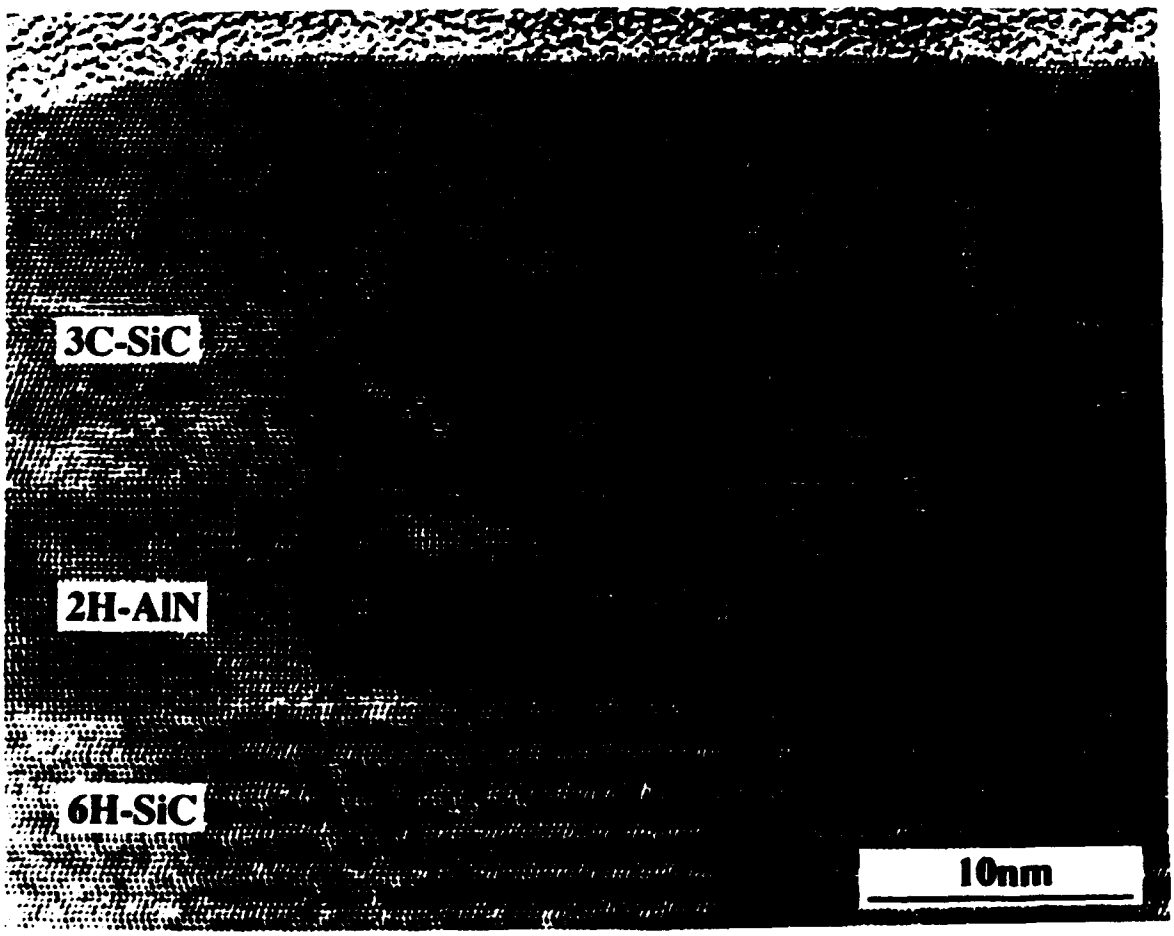

Figure 7. Cross-sectional HRTEM image of a multilayer with a 6H-SiC substrate, a 2H-AlN film, and a 3C-SiC film.

D. Discussion

1. Solid Solutions

As shown in Figs. 1 and 2, the solid solutions grown are AlN-rich, have a cubic crystal structure, and are polycrystalline. To the knowledge of the authors, this is the first cubic thin film solid solution in the $(AlN)_X(SiC)_{1-X}$ system. However, the polycrystalline nature of the film and the thinness prevent further characterization and analysis. Several techniques are presently being studied to improve the crystalline character of the films as well as the growth rate. This study should address all the variables in the growth procedure. In addition, the relative difficulty of carbon incorporation in these films must also be addressed. This is also being studied.

2. Multilayers

When the initial work was done on SiC (see previous reports), the optimum growth temperature was reported to be 1200-1250°C. These conditions were then attempted for AlN growth. The results are shown in Figure 3. The films showed poor interface and surface characteristics as described previously. The disordered interface can be lessened by holding the substrate for less time at temperature, thereby lessening any Si evaporation and/or surface roughening, and eliminating pre-exposure by the N_2 plasma which may result in Si_3N_4 formation. The rough interface indicates that the growth temperature is too high.

With these concerns in mind, the heterostructure shown in Figs. 4 through 7 was grown. The substrate temperature 1050°C (150°C lower), the substrate was not held at temperature for an extended period, and the substrate surface was carefully exposed to both Al and N to prevent Si_3N_4 formation at the interface. In addition, the SiC layer was grown at 1050°C.

As mentioned in the Introduction, many researchers have reported the growth of AlN on SiC substrates or SiC on AlN substrates. However, to the authors' knowledge, there has never been a report of a multilayer grown between these two materials as is presented here. In addition, there are no known reports of heterostructure growth where the first three layers (substrate included) each had a different crystal structure as presented here. This unique structure, made of direct (AlN) and indirect (SiC) wide bandgap materials, will have interesting mechanical, thermal, and electrical properties that should be studied. Also, the structure of the layers beyond those grown here will produce many interesting results. Future work is planned in these areas.

E. Conclusions

Cubic solid solutions of AlN and SiC were grown on off-axis 6H-SiC (0001) substrates by GSMBE. Although the films are polycrystalline, they represent the first thin film solid solutions in the SiC-AlN system. With better control and precision, single crystal films of high quality should be obtained.

The first AlN-SiC multilayer reported has also been presented and described herein. The layers of AlN and SiC are both single crystal and the interfaces are of good quality. A new substrate temperature, in the range where smooth, single crystal AlN can be grown, was found to produce single crystal SiC films. This multilayer is also the first reported to include three different crystal structures in its layers. With a smoother SiC surface, this structure can easily be extended to include more layers and even begin designing devices to exploit the structure properties.

F. Future Research Plans/Goals

Additional studies are planned to study the effect of substrate temperature on both the solid solutions and the multilayers. The resulting films will be analyzed chemically, structurally, and electrically to determine properties. Devices fabricated from pure materials, doped materials, solid solutions, and multilayers will also be studied.

G. References

1. G. R. Fisher and P. Barnes, Philos. Mag. B 61, 217 (1990).
2. H. P. Philipp and E. A. Taft, in *Silicon Carbide, A High Temperature Semiconductor*, edited by J. R. O'Connor and J. Smiltens (Pergamon, New York, 1960), p. 371.
3. W. von Muench and I. Pfaffender, J. Appl. Phys. 48, 4831 (1977).
4. E. A. Bergemeister, W. von Muench, and E. Pettenpaul, J. Appl. Phys. 50, 5790 (1974).
5. R. I. Skace and G. A. Slack, in *Silicon Carbide, A High Temperature Semiconductor*, edited by J. R. O'Connor and J. Smiltens (Pergamon, New York, 1960), p. 24.
6. W. von Muench and E. Pettenpaul, J. Appl. Phys. 48, 4823 (1977).
7. S. Nishino, Y. Hazuki, H. Matsunami, and T. Tanaka, J. Electrochem Soc. 127, 2674 (1980).
8. P. Das and K. Ferry, Solid State Electronics, 19, 851 (1976).
9. C. F. Cline and J. S. Kahn, J. Electrochem. Soc, 110, 773 (1963).
10. G. A. Slack, J. Phys. Chem. Solids 34, 321 (1973).
11. W. M. Yim, E. J. Stofko, P. J. Zanzucci, J. I. Pankove, M. Ettenberg, and S. L. Gilbert, J. Appl. Phys. 44, 292 (1973).
12. *Diamond, Silicon Carbide and Related Wide Bandgap Semiconductors*, J. T. Glass. R. Messier, and N. Fujimori, eds. (Mater. Res. Soc. Symp. Proc. 162, Pittsburgh, PA, 1990).
13. R. F. Davis, Z. Sitar, B. E. Williams, H. S. Kong, H. J. Kim, J. W. Palmour, J. A. Edmond, J. Ryu, J. T. Glass, and C. H. Carter, Jr., Mater. Sci. Eng. B 1,77 (1988).
14. *Properties of II-VI Semiconductors: Bulk Crystals, Epitaxial Films, Quantum Well Structures, and Dilute Magnetic Sytems*, edited by J. F. Schetzina, F. J. Bartoli, Jr., and H. F. Schaake(Mater. Res. Soc. Symp. Proc. 161, Pittsburgh, PA, 1990).
15. See, for example, R. Ruh and A. Zangvil, J. Am. Ceram. Soc. 65, 260 (1982).
16. W. R. L. Lambrecht and B. Segall, Phys. Rev. B 43, 7070 (1991).
17. T. L. Chu, D. W. Ing, and A. J. Norieka, Solid-State Electron. 10, 1023 (1967).
18. R. F. Rutz and J. J. Cuomo, in *Silicon Carbide-1973*, ed. by R. C. Marshall, J. W. Faust, Jr., and C. E. Ryan, Univ. of South Carolina Press, Columbia, p. 72 (1974).
19. M. E. Sherwin and T. J. Drummond, J. Appl. Phys. 69, 8423 (1991).
20. G. C. Osbourn, J. Vac. Sci. Technol. B 1, 379 (1983).
21. P. L. Gourley, R. M. Biefeld, G. C. Osbourn, and I. J. Fritz, *Proceedings of 1982 Int'l Symposium on GaAs and Related Compounds* (Institute of Physics, Berkshire, 1983), p. 248.

IV. Determination of the Diffusivity of the Al, Si, N and C at the Interface of the SiC-AlN Diffusion Couple

Abstract

The chemical interdiffusion of SiC and AlN is being investigated. For the initial run, a SiC-AlN diffusion couple was heated at 1500° C for 100 hours in a N_2 environment. Scanning Auger spectroscopy was employed for the measurements of the diffusion lengths of the four elements. The diffusivity of the four elements was calculated to be $\approx 10^{-14}$ cm^2/hr, which is about four orders of magnitude lower than the previously reported results.

A. Introduction

Several attempts have been made to alloy SiC with other compounds to control the mechanical and physical properties. Single crystal growth of SiC-AlN mixtures by epitaxial techniques on the SiC platelets is one example [1]. There exists a difference in opinion among investigators about the possibility of forming solid solutions or new phases in the SiC-AlN system at high temperatures [2]. The difficulties encountered in the attempts to obtain homogeneous SiC-AlN solid solutions are known to be related to the low diffusion coefficients.

The diffusion coefficients of N in SiC have been determined to be $\approx 10^{-12}$ cm^2/s at 2550° C [3]. In hot-pressed SiC-AlN samples and in SiC-AlN diffusion couples, approximate diffusion coefficients of SiC and AlN were calculated to be 1×10^{-12} cm^2/s [4]. The corresponding activation energy was roughly estimated to be as high as 900 kJ mol, and the pre-exponential term was $\approx 10^{-8}$ cm^2/s which is an unusually high value. Thus, it was suggested that lattice diffusion of coupled SiC and AlN pairs was responsible for these high values.

Phase transformations in the SiC-AlN system have also been studied. The 3C→2H transformation was observed to proceed through a heavily faulted cubic structure which contained up to 4 % AlN [4].

In this investigation, the diffusion coefficient and the corresponding activation energy for the diffusion of the four elements Si, C, Al, and N in the interface layer between the single crystal SiC and sintered AlN materials will be determined. Although the diffusion coefficients for N in SiC at high temperature have been determined previously, the atomic behavior and phase formation at relatively low temperature for thin film deposition have not been yet clarified For this experiment, Auger spectroscopy and TEM will be employed to determine the nature and extent of the diffusion profiles and the existence (or lack of it) of additional phases in the solid solution region and at the interfaces between the solution and the end-member phases.

B. Experimental Procedures

A SiC sample was prepared from a single crystal wafer manufactured by Cree Research, Inc. The AlN sample was prepared from sintered bulk material. The SiC wafer was used in the as-received condition, since the surface was already polished. The preparation of the AlN specimen was performed using a lapping machine in which the sample is rotated on the glass plate. For the lapping of the sample, 30 micron, 6 micron 1 micron and 0.1 micron diamond slurries were used. The polished surface of the SiC and AlN was joined just before setting into the furnace for the diffusion. The sample is heated initially to 1150°C and held there for 30 minutes under a pressure of 20 psi. After releasing the load, the temperature of the furnace is raised to 1500°C. After the diffusion anneal, the sample was lapped at an angle of 34° to determine the scanning concentration profile by Auger spectroscopy. This produced a magnification of the interface between the two materials of ≈100 times. Depth concentration profiles were taken on an island of the SiC remaining on the AlN layer. The difference in the reflectivity of the two materials makes it easier to determine the interface area in the Auger equipment.

C. Results

The depth profiles of the concentration of the four elements for this initial sample are shown in Figure 1. The data in Figure 1 are too inaccurate to calculate the diffusivity of the four elements. This is due to the rough interfaces and surface of the sputtered area. All the profiles in the Figure 1 are as expected except the oxygen profile. Oxygen is not expected to be present in the SiC or AlN materials. However, the concentration of the oxygen increases toward the AlN side. The oxide film is formed on the angle lapped surface of SiC. With ion sputtering of the surface, the oxide layer is easily eliminated, as can be seen in the Figure 1. In order to confirm this concentration depth profile, line scanning across the diffused region was conducted as the results can be seen in Figures 2–5. Using these data from the depth profiles, the diffusivity of the four elements near the interface of the SiC and AlN can be roughly estimated using the equation:

$$c(x,t) = (c/2)\,[\,1 - \mathrm{erf}\,\{x / 2\,(Dt)^{1/2}\}\,] \quad (1)$$

The results of this calculation are shown in the Table I. In this calculation, the diffusivity is assumed to be constant. However, as can be seen in the Table I, the diffusivity seems to be varied depending on the position. The diffusivities calculated in this preliminary experiment are about four orders of magnitude lower than the results of Zangvil or Vodakov.

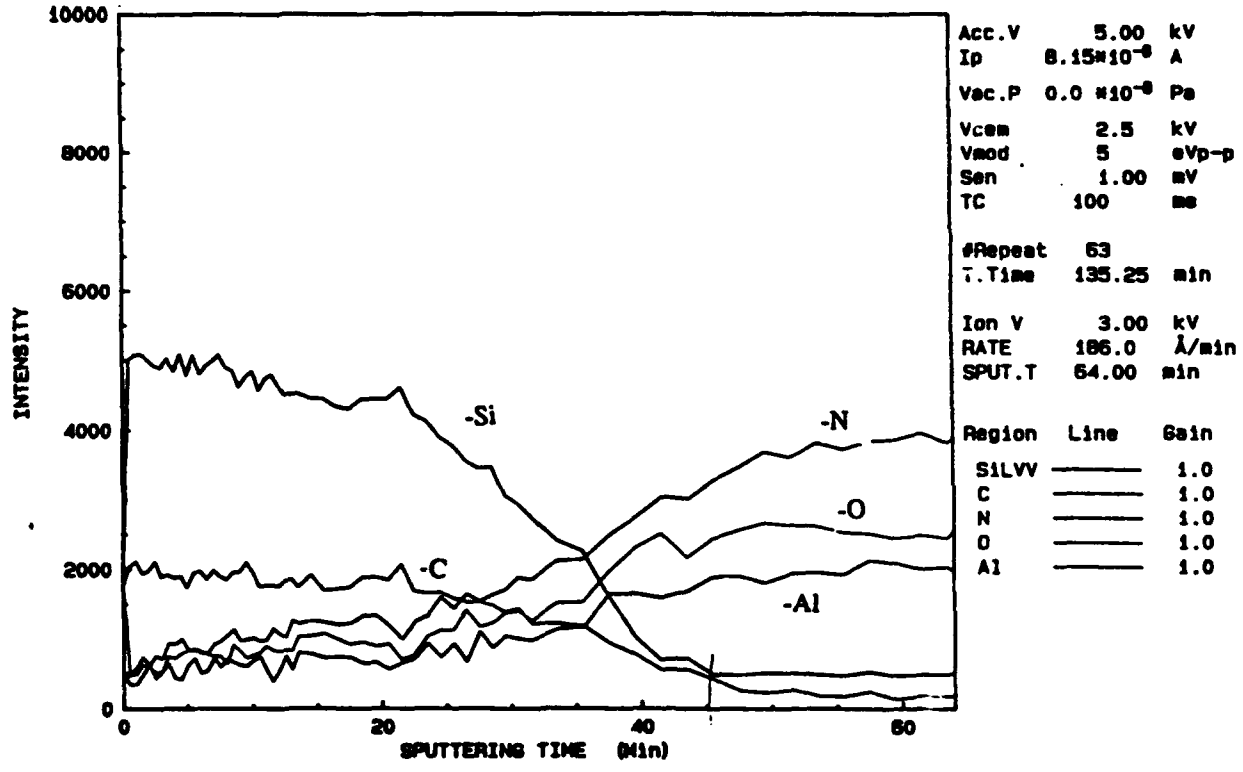

Figure 1. Depth concentration profile at the interface of SiC and AlN.

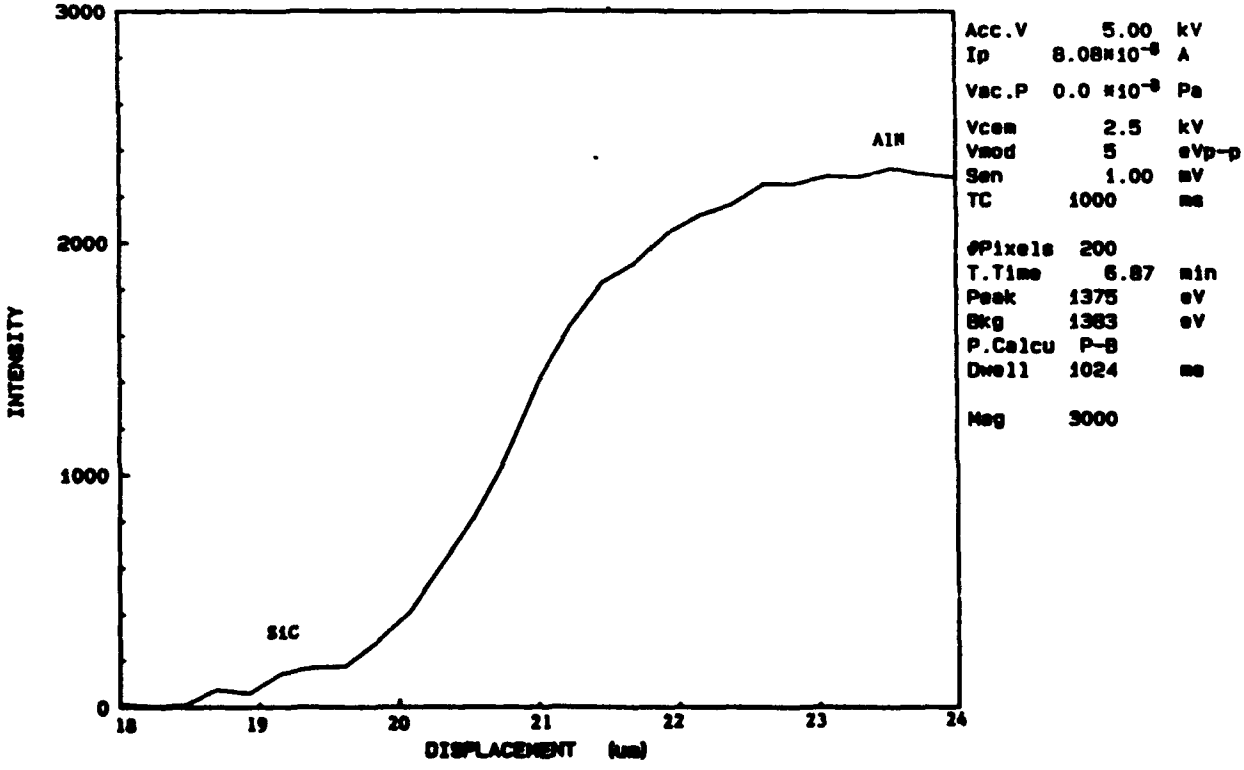

Figure 2. Line scanning of the Al concentration at the interface of SiC and AlN.

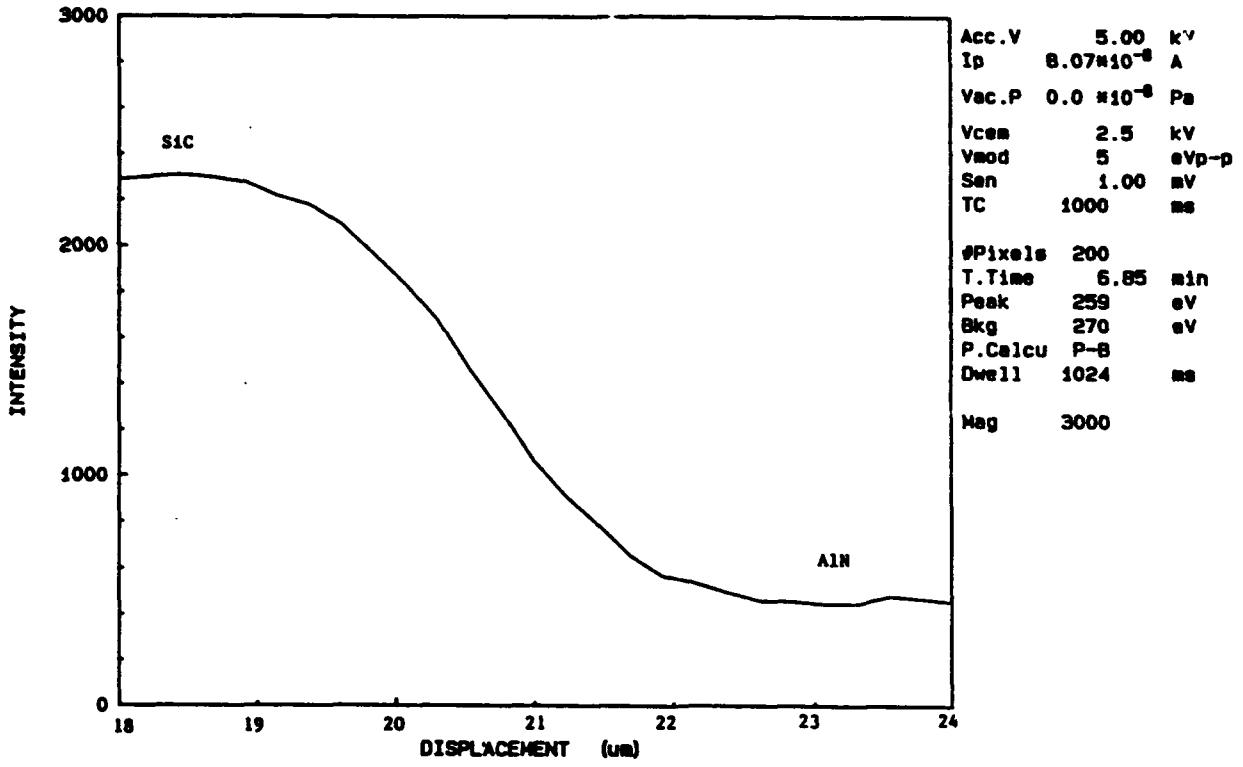

Figure 3. Line scanning of the C concentration at the interface of SiC and AlN.

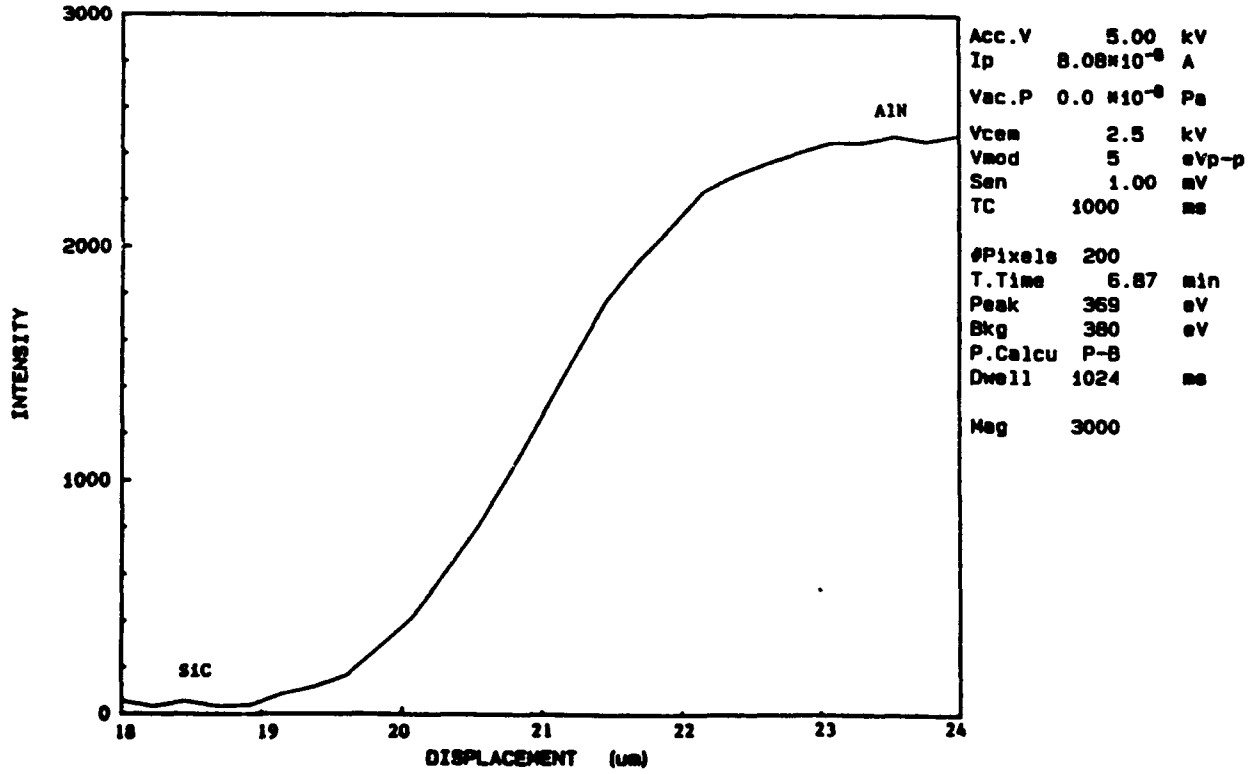

Figure 4. Line scanning of the N concentration at the interface of SiC and AlN.

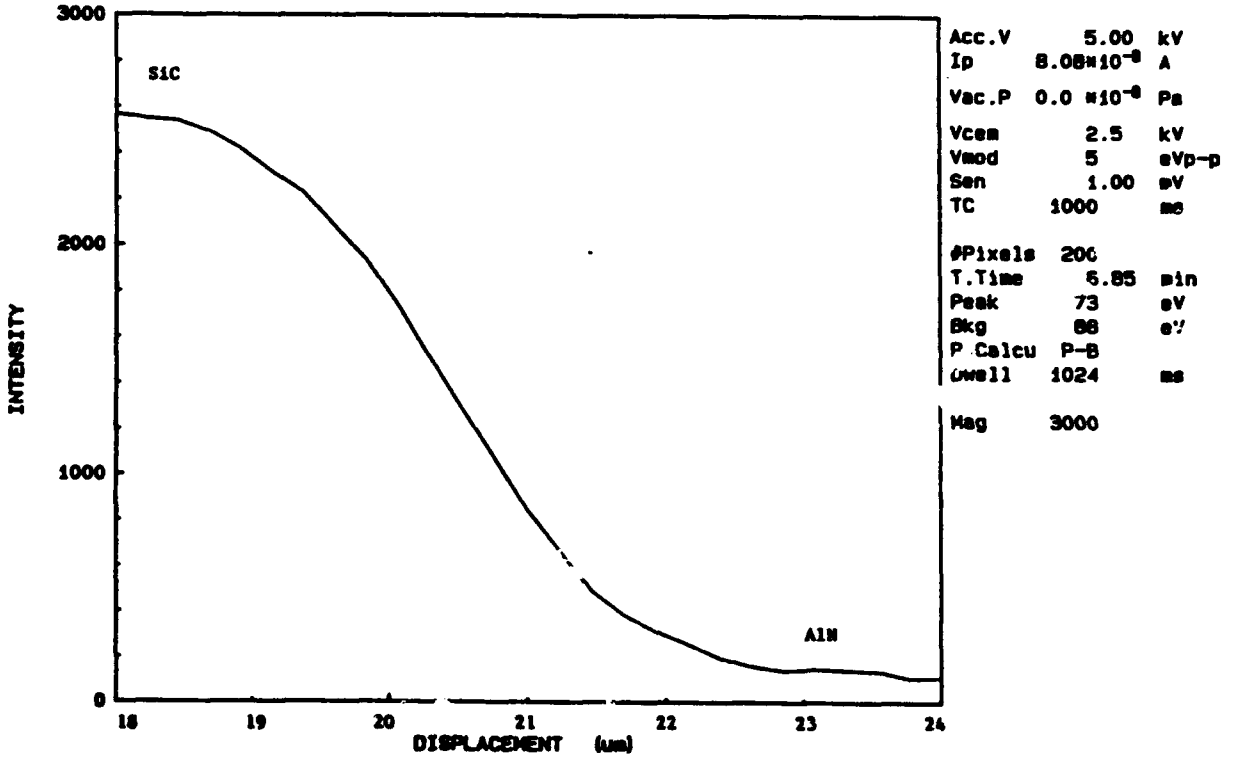

Figure 5. Line scanning of the Si concentration at the interface of SiC and AlN.

Table I.

Diffusivity (10^{-14} cm ^{2} / hr)	in AlN	in SiC
Silicon	7.96	8.4 -8.6
Carbon	6.7 - 7.3	.4-4.7
Aluminum	11	5.29
Nitrogen	6.8	5.76-6.76

D. Discussion

As can be seen in Figure 1, the depth concentration profile is too rough for the determination of the diffusivity. This may be due to the poor preparation of the raster by the ion gun. It indicates that the sputtered area should be larger and sufficiently flat for more accurate measurement of the depth profile of the concentration. The actual sputtering rate in SiC and AlN should be measured at the same time. Once an accurate depth profile is obtained, it seems to be very useful to estimate the diffusion depth. As can be seen in Figure 6, the angle-lapped interface of the AlN and SiC is not so sufficiently smooth to obtain

concentration profiles by scanning technique. This rough interface would result in unreliable data in the Auger scanning technique if one is not careful in selecting the scanning position in the specimen. Thus, for a more accurate determination of the concentration profile near the interface of the two materials, depth profile and line scanning technique should be employed at the same time.

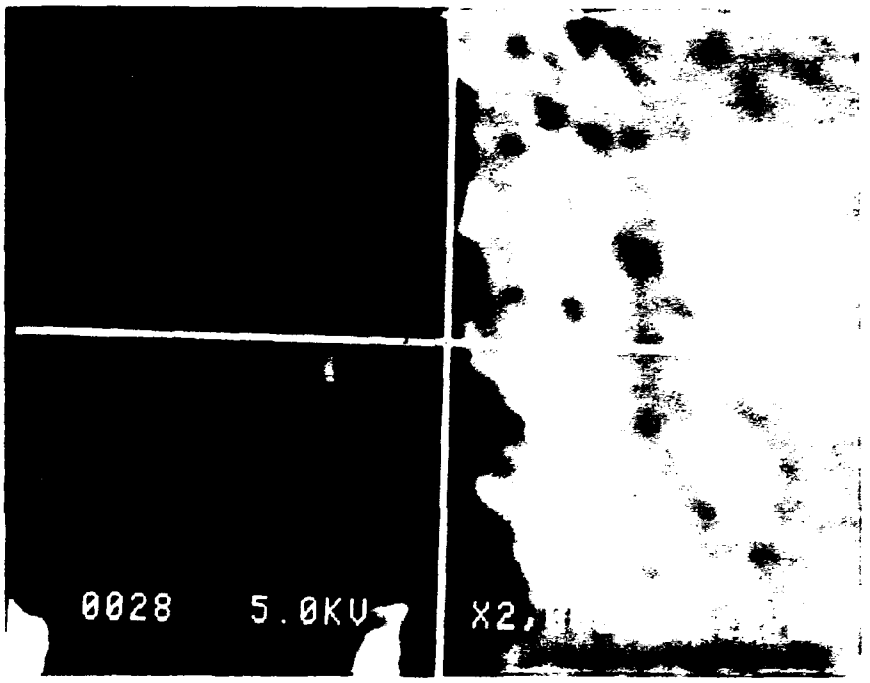

Figure 6. SEM picture of the angle-lapped surface of the SiC and AlN interface.

Zangvil and Ruh calculated approximate diffusion coefficients of SiC in AlN as 1×10^{-12} $cm^2 s^{-1}$ at 1950 ° C [4]. This value is very high compared to the diffusivities in Table I. There is about four orders of magnitude difference between them. It was suggested that the lattice diffusion of coupled Al-N and Si-C pairs was responsible for these high values. However, according to the data in the Table I, there are some differences in the diffusivity between Si and C or Al and N. These differences in the diffusivity suggest that the atoms diffuse individually at low temperatures although pair mechanisms may be operative at high temperature. As can be seen in the Table I, the diffusivity of each element varies depending on the position. This may indicate the necessity of the employment of the Boltzmann's method in the accurate determination of the diffusivity for the four elements. However, no distinct break of the concentration across the interface is observed for any of the four elements. It seems that the surface condition of the two materials is smooth and sufficiently

clean for the atoms to cross the interface without additional difficulty. The higher diffusivity of carbon in AlN than in SiC may indicate a grain boundary contribution in the AlN. These results confirm that the materials selection and the sample preparation procedure employed in this experiment are sufficiently good to provide reliable data.

E. Conclusions

1. The diffusivity of the four elements at the interface of the SiC-AlN at 1500° C is roughly calculated as 10^{-17} cm^2/s at 1500° C. This is about four orders of magnitude lower than the previous calculations at higher temperature.
2. No major problem has been found in the selection and in the sample preparation procedure employed in this experiment. However, for more accurate determination of the diffusivity with Auger spectroscopy, a wider raster is desirable in the depth concentration profile.

F. Future Plans

1. Determine the temperature dependence of the diffusivity via the use of diffusion anneals at 1500, 1550, 1600, 1650 and 1700° C will be tried.
2. At each of these temperatures, the anneals will be conducted for two different times, 50 hours and 200 hours for more accurate determination of the diffusivity.
3. To determine the existence of any new phases near the interface of the two materials, TEM will be employed.

G. References

1. W. F. Knippenberg et al., U.S. Patent No. 3,634,149, 1972.
2. N. D. Sorokin, Yu. M. Tairov, and V. F. Tsvetkov, "Study of the Composition of Solid Solution SiC-AlN and SiC-GaN by the Method of X-ray Spectral Analysis," p.227 in *Abstracts of Reports at the Third All-Union Symposium on Scanning Electron Microscopy and Analytic Methods for Studying Solids*, Zvenigorod. Nauka, Moscow, 1981.
3. Y. A. Vodakov, and E.N. Mokhov, "Diffusion and Solubility of Impurities in Silicon Carbide," pp. 508-19 in Silicon Carbide-1973, edited by R. C. Marshall, J. W. Faust, Jr., and C. E. Ryan, University Press, S. C., 1974.
4. A. Zangvil and R. Ruh, J. Mat. Sci. and Engr. 71 159 (1985).

V. Deposition of Cubic Boron Nitride on Diamond

A. Introduction

A significant effort has also been initiated to produce pseudomorphic cubic-BN layers on diamond substrates. The converse deposition will also be studied in the near future.

B. Experimental Procedures

1. Film Growth

A UHV ion beam assisted deposition (IBAD) system was used for film deposition. Samples were loaded through a load lock system. Base pressures in the chamber were typically $< 1 \cdot 10^{-9}$ Torr. Boron was deposited by evaporating boron metal using an electron beam evaporator. Simultaneously a Kaufman type ion gun was used to bombard the depositing boron with both nitrogen and argon ions. The films were deposited onto heated substrates. A schematic of the setup is shown in Figure 1. The deposition rate of the boron, the energy and flux of the ions, the ratio of the argon to nitrogen, and the substrate temperature were all measured, controlled, and varied. The boron was evaporated using a Thermionics HM2 electron gun with an electromagnetic beam sweep. The boron was in a graphite crucible liner which was in a water cooled 10 cc crucible. It was deposited at a rate of from 0.25 to 1.0 Å/s. The deposition rate was monitored using a quartz crystal monitor.

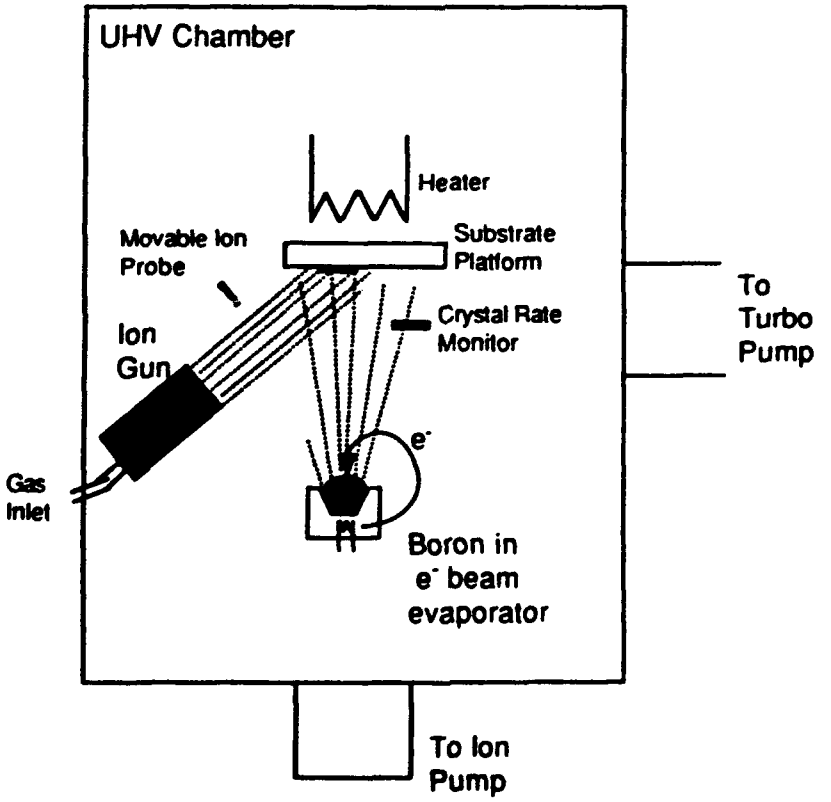

Figure 1. Schematic of electron beam MBE deposition system.

The film was bombarded using an Ion Tech 3 cm Kaufman ion source. Bombardment was by either nitrogen and argon or nitrogen and krypton ions in varied ratios, all at 500 eV. The flux of ions ranged from 0.05 to .30 mA/cm^2 and was measured using a negatively biased ion probe. The gas flow to the ion gun was 1.5 sccm for each of the two gases and was controlled using MKS mass flow controllers. Typical deposition pressures in the chamber were 1.0×10^{-4} Torr.

The diamond films were grown using a microwave CVD process with 1% CH_4 and were 2–4 μm thick. Before the c-BN deposition the substrates with the diamond films were etched in boiling H_2SO_4:HNO_3:$HClO_4$ solution in the ratio of 3:4:1 for 45 minutes to remove any graphite phase. A 500 Å BN film was then deposited on the diamond film at 400°C.

2. Film Characterization via FTIR

Fourier transform infrared spectroscopy (FTIR) has been found to be the best method for the purpose of determining whether a deposited film is cubic or hexagonal boron nitride. With FTIR analysis the cubic and hexagonal forms of boron nitride give distinct, independent peaks, due to the sp^3 and sp^2 bonds, respectively. Hexagonal boron nitride has absorption peaks at 1367 cm^{-1} and at 783 cm^{-1} [1], while cubic boron nitride has a transverse optical mode absorption peak at 1075 cm^{-1} [2].

C. Results

An FTIR spectrum for one of these films is shown in Figure 2. It is seen that the c-BN peak is present, and there is no evidence of an h-BN peak. Unfortunately the signal to noise ratio is very low, so the pattern is not very clear. This may be due to the small area of the substrates (~1 cm^2). Depositions are presently being conducted on other diamond films, and we hope to get clearer results from those depositions.

D. Discussion

The results from depositing on the diamond films indicate that cubic boron nitride will grow on diamond. The present thrust of our research is deposition on diamond, and optimizing the conditions for c-BN on diamond growth.

E. Conclusions

Depositions on diamond thin films have been done, and preliminary results show the growth of c-BN with little or no other phases present.

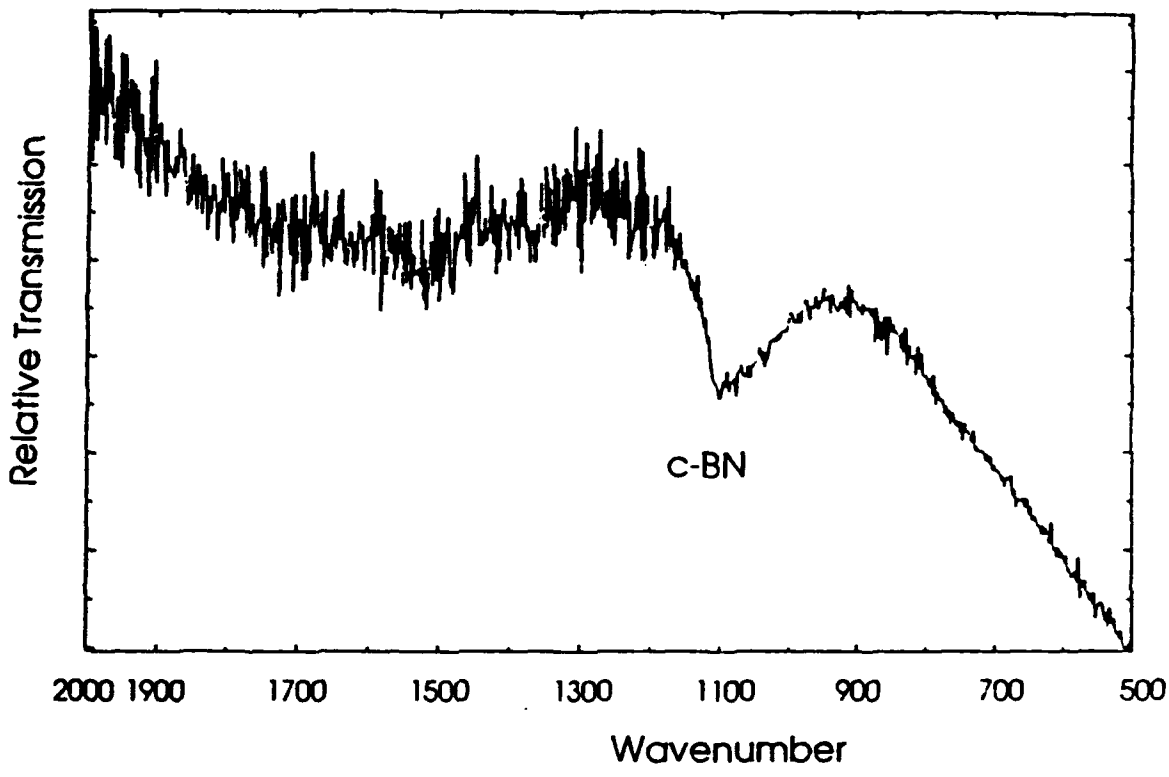

Figure 2. FTIR spectra of BN film deposited on diamond thin film on a silicon substrate. Deposition conditions: Boron deposition rate: 0.5 Å/s; ion energy: 500 eV; ion flux: 0.24 mA/cm^2; ion bombardment by 50:50 Ar:N_2; substrate temp: 400°C; film thickness: 500Å.

F. Future Research Plans/Goals

The goal of this research is to grow cubic boron nitride films of sufficient quality that they may be used for electronic applications. Due to its properties including very high band gap and high thermal stability and thermal conductivity, cubic boron nitride has the potential of being an excellent material for high power and high temperature devices. To make c-BN films of electronic device quality will require several things. The first is an improvement in the relative phase ratio (cubic to non-cubic phases). Ideally, films would be 100% cubic.

A second requirement for electronic quality c-BN is to maximize grain size. Ideally this would mean single crystal films. Grain size needs to be maximized in order to minimize the area of grain boundaries which degrade the electrical properties of a film by acting as recombination sites, can be electrically active, are high diffusion paths, and are areas where concentrations of impurities may occur.

The third requirement is to minimize impurities in the films, which can act as scattering centers, and may be electrically active.

Depositions on diamond films will be emphasized. It is expected that diamond will be an excellent substrate for cubic boron nitride deposition due to the close lattice matching

between diamond and c-BN, the good thermal expansion match, and the fact that diamond has a higher surface energy than c-BN. We have a broad range of diamond films available, deposited using various techniques from several sources. We will try to both optimize the conditions necessary for c-BN growth on diamond, as well as comparing the growth on diamond films prepared using different deposition conditions to see how that affects the c-BN growth.

As film quality improves, characterization emphasis will shift towards electrical measurements. As the deposition process is modified, with corresponding changes in film phase, and film impurity content, the effect on electrical properties will be closely monitored. Measurements will include I-V, C-V, 4-point probe, and Hall effect measurements.

G. References

1. J. Thomas, Jr., N. E. Weston, and T. E. O'Conner, J. Am. Chem. Soc. **84**, 4619 (1963).
2. R. H. Wentorf, Jr., J. Chem. Phys. **26**, 956 (1957).

VI. Distribution List

	Number of Copies
Mr. Max Yoder Office of Naval Research Electronics Division, Code: 1114SS 800 N. Quincy Street Arlington, VA 22217-5000	3
Administrative Contracting Officer Office of Naval Research Resident Representative The Ohio State University Research Center 1314 Kinnear Road Columbus, OH 43212-1194	1
Director Naval Research Laboratory ATTN: Code 2627 Washington, DC 20375	1
Defense Technical Information Center Bldg. 5, Cameron Station Alexandria, VA 22314	12